Borneo Journal of Resource Science and Technology (2023), 13(2): 161-174
DOI: https:doi.org/10.33736/bjrst.5935.2023

Synthesis, *in vitro* and *in silico* Studies of Alkylated Paracetamol Derivatives as Potential Antibacterial Agent

AINAA NADIAH ABD HALIM*, AINA SYAKIRAH MOHAMMAD HUSSIN, ZAINAB NGAINI, NGIENG NGUI SING, STEPHANIE ALMA JONG & MUHAMMAD MUQRI MOHAMAD SABERI

Faculty of Resource Science and Technology, Universiti Malaysia Sarawak, 94300 Kota Samarahan, Sarawak, Malaysia
*Corresponding author: ahanadiah@unimas.my
Received: 9 August 2023 Accepted: 4 December 2023 Published: 31 December 2023

ABSTRACT

In the field of drug development, structural modification of over-the-counter drugs is extensive to combat drug-resistant strains as well as discover new purposes or biological applications. Paracetamol is an example of OTC analgesic drug that is commonly used in the treatment of pain and fever. In this research, paracetamol was modified by introducing various alkyl chains C_nH_{2n+1}, where n varied from 3 to 14 *via* Williamson etherification with bromoalkanes to yield 49% – 86% of *N*-(4-oxy)phenyl)acetamide derivatives **1**-**10**. Employing the Kirby-Bauer disc diffusion method, the bacteriostatic activity of the series in comparison to the parental compound (paracetamol) and standard drug (ampicillin) showed that compounds **1** (n = 3), **4** (n = 6) and **7** (n = 9) displayed excellent activity against *Escherichia coli* with an inhibition zone of 8.1 ± 0.4 mm, 8.3 ± 0.4 mm and 7.9 ± 0.5 mm, respectively, while the paracetamol and ampicillin inhibition zones are 8.0 ± 0.0 mm and 16.0 ± 0.0 mm, respectively. Interestingly, compounds **7** (n = 9) and **10** (n = 14) exhibited excellent activity towards *Staphylococcus aureus* with an inhibition zone of 8.2 ± 0.4 mm and 12.5 ± 0.5 mm, respectively, outperforming paracetamol (6.0 ± 0.0 mm) and ampicillin (11.0 ± 0.0 mm). The *in vitro* findings were in line with the molecular docking investigation conducted using AutoDock Vina software towards the active site of DNA gyrase enzymes, revealing the structure-activity relationship of the series. Besides, the synthesised compounds **1-10** complied with the drug-likeness analysis and ADME pharmacokinetics profile. The results of this study are significant in delivering new prospects of the potential antibacterial drugs obtained through derivatisation of the known drug, paracetamol. While these initial results are promising, further toxicity and *in vivo* analyses are necessary to ensure the efficacy and safety of the newly developed drug in living organisms, providing a clearer understanding of its potential as an antibacterial medicine.

Keywords: 4-Acetaminophen, ADME, bacteriostatic agent, molecular docking, Williamson etherification

INTRODUCTION

With the recent experience of the pandemic, the emergence of new drugs has become a priority due to the spiking cases of infectious diseases caused by antimicrobial resistance. In the drug discovery and development process, structure-based drug design is essential to ensure the effectiveness and efficiency of the drugs towards the target receptor (Batool *et al*., 2019). The conventional way of identification and development of new therapeutic drugs takes 12-15 years with a cost between $900 million to $2 billion from the point of formulation to the point of drug approval (Deore *et al*., 2019). However, given the current circumstance, the urgency has forced the researchers to turn to different strategies that could expedite the process while delivering similar effectiveness. The innovative strategies that are being conducted intensively by the researchers are performing repurposing, repositioning, redirecting and modifying the over-the-counter approved drugs (Farha & Brown, 2019; Moo *et al*., 2019) on top of computational tools that assist in escalating the drug discovery process by giving information of the drugs pharmacokinetic and pharmacodynamics (Barbolosi *et al*., 2016).

Paracetamol or also known as *N*-(4-hydroxyphenyl) ethanamide are widely used drug that was first synthesised in 1878 by Morse and used as an analgesic (pain reliever) and antipyretic (reduce fever) in the medical field

since 1893 (Przybyła *et al*., 2021). The chemical structure of paracetamol comprises of a benzene ring, a hydroxyl group and an amide group located at the *para* position (Refat *et al*., 2017; Srabovic *et al*., 2017) allowing further structural modification and capable to serve as precursors for a formation of new derivatives (Begum *et al*., 2023*)*. There are previously reported studies on the modification of paracetamol for various biological applications (Begum *et al*., 2023) for instance, antioxidant (Alisi *et al*., 2012; Sathe *et al*., 2019), antitubercular (Ahmad *et al*., 2016), anticancer (Ramanjaneyulu *et al*., 2019) and antibacterial activities (Kumar *et al*., 2018).

Owing to the structure of paracetamol, the modifications are advancing at a significant pace in which, in this context, the presence of the phenolic hydroxyl group enabled the formation of ether through Williamson etherification which occurs via SN_2 reaction by deprotonation of an alkoxide ion which further reacted with a primary alkyl halide for the addition of alkyl substituents (Long *et al*., 2020; Yearty *et al*., 2020). The interest in the introduction of alkyl substituents into the structure is based on previous studies and literature precedents that reported the presence of long alkyl chains could contribute to a better antimicrobial effect (Abd Halim & Ngaini, 2016; Ardean *et al.*, 2021; Odžak *et al*., 2023). This is due to the amphiphilic properties of the compounds possessing both hydrophobicity and lipophilicity character improving the adhesion to the bacterial cell membrane which eventually leads to disruption (Sahariah *et al*., 2015; Babamale *et al*., 2021; Mehta *et al*., 2021). Furthermore, compounds containing an alkyl chain in their structure can imitate the membrane of the bacterial cell wall, increasing its permeability and inflicting damage reflected by an increase in the bactericidal action (Mehta *et al*., 2021; Gao *et al*., 2022; Lin *et al*., 2023).

Hence, herein we report on the synthesis of *N*-(4-oxy)phenyl)acetamide derivatives **1-10** modified from paracetamol as parent structures bearing alkyl chains C_nH_{2n+1}, where n varied from 3 to 14. The series was evaluated for its antibacterial potential against both Gram-negative (*Escherichia coli*) and Gram-positive bacteria (*Staphylococcus aureus*) where the effects of the alkyl chains lengths were evaluated followed by a discussion on the structure-activity relationship (SAR) obtained through docking and pharmacokinetics profile from absorption, distribution, metabolism and excretion (ADME) analysis.

MATERIALS AND METHODS

Chemicals

4-Hydroxyacetanilide (paracetamol), sodium hydroxide, 1-bromopropane (C_3), 1-bromobutane (C_4), 1-bromopentane (C_5), 1-bromohexane (C_6), 1-bromoheptane (C_7), 1-bromooctane (C_8), 1-bromononane (C_9), 1-bromodecane (C_{10}), 1-bromododecane (C_{12}), and 1-bromotetradecane (C_{14}) were acquired from Merck. Potassium carbonate was purchased from Fisher Scientific. The acetone solvent was dried and distilled over calcium hydride under nitrogen prior to usage while all the other reagents were used as received without any further purification.

Equipments or Instrumentations

Melting points were determined using Stuart SMP3 melting point apparatus and uncorrected. The elemental CHNS analysis was conducted using the Thermo Scientific FlaskSmart Elemental Analyzer. Infra-red (IR) spectra (ν/cm^{-1}) were recorded at the wavelength of 400 – 4000 cm^{-1} with KBr pellets on Perkin Elmer 1605 spectrophotometer. ^{1}H NMR and ^{13}C NMR spectra were recorded using JEOL ECA 500 spectrometer at 500MHz (^{1}H) and 125 MHz (^{13}C) with the chemical shifts δ (ppm) reported relative to chloroform-d ($CDCl_3$) as standards.

General Synthesis Procedure of *N*-(4-oxy)phenyl)acetamide derivatives, 1-10

In 20 mL of acetone, a mixture of 4-hydroxyacetanilide (3 mmol), alkyl bromide (3 mmol) and K_2CO_3 (0.41 g, 3 mmol) was heated at reflux with constant stirring for 48 h. The reaction mixture was brought to dryness after being cooled to room temperature. The solid obtained was then agitated for one hour with 50 mL of 2% sodium hydroxide and filtered to afford N-(4-oxy)phenyl)acetamide derivatives **1–10** with the following yields.

***N*-(4- propoxyphenyl)acetamide (1)**. Compound **1** was obtained as a white solid**.** Yield: 0.35 g (60.0%), m.p: 107 – 108 °C; (Found: C, 68.40; H, 7.87; N, 7.26. $C_{11}H_{15}NO_2$. Requires: C, 68.37; H, 7.82; N, 7.25); ν_{max} (KBr/

cm^{-1}) 3254 (N-H), 2933 (C-H), 1655 (C=O),1506 (Ar-C), 1020 (C-O). δ_H (500 MHz, $CDCl_3$) 1.0 (3H, t, 1x CH_3), 1.7–1.9 (3H, m, CH_2CH_3), 3.90 (2H, t, 1x OCH_2), 6.8 (2H, 10 d, *J* = 7.65 Hz, Ar-H), 7.4 (2H, d, *J* = 8.6 Hz, Ar-H), 7.3 (1H, s, 1x NH). δ_C (125 MHz, $CDCl_3$) 10.6 (CH_3), 22.7, 24.4 (CH_2), 69.9 (O-CH_2), 114.9, 122.0, 130.8, 156.1 (Ar-C), 168.4 (C=O).

***N*-(4-butoxyphenyl)acetamide (2)**. Compound **2** was obtained as a white solid. Yield: 0.37 g (59.7%), m.p: 111-112 °C; (Found: C, 69.59; H, 8.29; N, 6.79. $C_{12}H_{17}NO_2$. Requires: C, 69.54; H, 8.27; N, 6.76); ν_{max} (KBr/ cm^{-1}) 3304 (N-H), 2935 (C-H), 1657 (C=O), 1509 (Ar-C), 1024 (C-O). δ_H (500 MHz, $CDCl_3$) 1.0 (3H, t, 1x CH_3), 1.6 – 1.8 (5H, m, CH_2CH_3), 3.9 (2H, t, 1x OCH_2) , 6.8 (2H, d, *J* = 7.65 Hz, Ar-H), 7.4 (2H, d, J = 8.6 Hz, Ar-H), 7.2 (1H, s, 1x NH). δ_C (125 MHz, $CDCl_3$) 13.9 (CH_3), 19.3, 24.4, 31.4, 68.1 (O-CH_2), 114.9, 122.0, 130.8, 156.1 (Ar-C), 168.3 (C=O).

***N*-(4-pentyloxyphenyl)acetamide (3)**. Compound **3** was obtained as a white solid. Yield: 0.53 g (79.1%), m.p: 107 – 108 °C; (Found: C, 70.58; H, 8.62; N, 6.33. $C_{13}H_{19}NO_2$. Requires: C, 70.56; H, 8.65; N, 6.33); ν_{max} (KBr/ cm^{-1}) 3325 (NH), 2955 (CH), 1658 (C=O), 1514 (Ar-C), 1029 (C-O). δ_H (500 MHz, $CDCl_3$) 1.0 (3H, t, 1x CH_3), 1.6 – 1.8 (7H, m, CH_2CH_3), 3.9 (2H, t, 1x OCH_2), 6.8 (2H, d, *J* = 7.65 Hz, Ar-H), 7.4 (2H, d, *J* = 8.6 Hz, Ar-H), 7.3 (1H, s, 1x NH). δ_C (125 MHz, $CDCl_3$) 14.1 (CH_3), 22.5, 24.4, 28.3, 29.0, 68.4 (O-CH_2), 144.9, 122.0, 130.8, 156.1 (Ar-C), 168.4 (C=O).

***N*-(4-(hexyloxy)phenyl)acetamide (4)**. Compound **4** was obtained as a white solid. Yield: 0.45 g (51.1%), m.p: 111 – 112 °C; (Found: C, 71.46; H, 8.95; N, 5.92. $C_{14}H_{21}NO_2$. Requires: C, 71.46; H, 8.99; N, 5.95); ν_{max} (KBr/ cm^{-1}) 3282 (NH), 2939 (CH), 1655 (C=O), 1507 (Ar-C), 1029 (C-O). δ_H (500 MHz, $CDCl_3$) 0.9 (3H, t, 1x CH_3), 1.25 – 1.76 (6H, m, 3xCH_2), 2.16 (3H, s, 1xCH_3), 3.86 (2H, t, 1x OCH_2), 6.86 (2H, d, *J* = 7.65 Hz, Ar-H), 7.42 (2H, d, J = 8.6 Hz, Ar-H), 7.31 (1H, s, 1x NH). δ_C (125 MHz, $CDCl_3$) 14.1 (CH_3), 22.7, 24.4, 25.8, 29.3, 31.7, 68.4 (O-CH_2), 114.8, 122.0, 130.8, 156.1(Ar-C), 168.4 (C=O).

***N*-(4-(heptyloxy)phenyl)acetamide (5)**. Compound **5** was obtained as a white solid. Yield: 0.37 g (49.0%), m.p: 99 – 100 °C; (Found: C, 72.10; H, 9.30; N, 5.65. $C_{15}H_{23}NO_2$. Requires: C, 72.25; H, 9.30; N, 5.62); ν_{max} (KBr/ cm^{-1}) 3295 (NH), 2925 (CH), 1655 (C=O), 1511 (Ar-C), 1016 (Ar-O). δ_H (500 MHz, $CDCl_3$) 0.8 (3H, t, 1x CH_3), 1.25 – 1.77 (8H, m, 4xCH_2), 2.10 (3H, s, 1xCH_3), 3.91 (2H, t, 1x OCH_2), 6.81 (2H, d, *J* = 7.0 Hz, Ar-H), 7.35 (2H, d, *J* = 7.0 Hz, Ar-H), 7.63 (1H, s, NH). δ_C (125 MHz, $CDCl_3$) 14.1 (CH_3), 22.7, 24.3, 26.1, 28.9, 29.1, 31.8, 68.4 (O-CH_2), 114.8, 115.2, 122.0, 130.9, 156.1 (Ar-C), 168.5 (C=O).

***N*-(4-(octyloxy)phenyl) acetamide (6)**. Compound **6** was obtained as a white solid. Yield: 0.47 g (59.0%), m.p: 99 – 100 °C; (Found: C, 72.96; H, 9.53; N, 5.32. $C_{16}H_{25}NO_2$. Requires: C, 72.96; H, 9.57; N, 5.32); ν_{max} (KBr/ cm^{-1}) 3318 (NH), 2925 (CH), 1655 (C=O), 1508 (Ar-C), 1033 (Ar-O). δ_H (500 MHz, $CDCl_3$) 0.88 (3H, t, 1x CH_3), 1.25 – 1.77 (12H, m, 6xCH_2), 2.16 (3H, s, 1xCH_3), 3.94 (2H, t, 1x OCH_2), 6.87 (2H, d, *J* = 8.5 Hz, Ar-H), 7.32 (2H, d, *J* = 6.5 Hz, Ar-H), 7.38 (1H, s, NH). δ_C (125 MHz, $CDCl_3$) 14.1 (CH_3), 22.7, 24.4, 26.1, 29.3, 29.3, 29.4, 31.9, 68.4 (O-CH_2), 114.8, 122.0, 130.7, 156.1 (Ar-C), 168.5 (C=O).

***N*-(4-(nonyloxy)phenyl) acetamide (7)**. Compound **7** was obtained as a white solid. Yield: 0.62 g (75.0%), m.p: 99 – 100 °C; (Found: C, 73.64; H, 9.79; N, 5.02. $C_{17}H_{27}NO_2$. Requires: C, 73.61; H, 9.81; N, 5.05); ν_{max} (KBr/ cm^{-1}) 3290 (NH), 2919 (CH), 1656 (C=O), 1507 (Ar-C), 1018 (Ar-O). δ_H (500 MHz, $CDCl_3$) 0.88 (3H, t, 1x CH_3), 1.25 – 1.78 (14H, m, 7xCH_2), 2.11 (3H, s, 1xCH_3), 4.04 (2H, t, 1x OCH_2), 6.83 (2H, d, *J* = 6.5 Hz, Ar-H), 7.36 (2H, d, *J* = 7.0 Hz, Ar-H), 7.42 (1H, s, NH). δ_C (125 MHz, $CDCl_3$) 14.2 (CH_3), 22.8, 24.3, 26.1, 29.3, 29.3, 29.4, 29.6, 31.9, 68.4 (O-CH_2), 114.8, 122.0, 130.9, 156.1 (Ar-C), 168.5 (C=O).

***N*-(4-(decyloxy)phenyl) acetamide (8)**. Compound **8** was obtained as a white solid. Yield: 0.75 g (86.0%), m.p: 100 – 101 °C; (Found: C, 74.14; H, 10.02; N, 4.79. $C_{18}H_{29}NO_2$. Requires: C, 74.18; H, 10.03; N, 4.81); ν_{max} (KBr/ cm^{-1}) 3307 (NH), 2922 (CH), 1657 (C=O), 1508 (Ar-C), 1020 (Ar-O). δ_H (500 MHz, $CDCl_3$) 0.88 (3H, t, 1x CH_3), 1.25 – 1.76 (16H, m, 8xCH_2), 2.16 (3H, s, 1xCH_3), 3.92 (2H, t, 1x OCH_2), 6.87 (2H, d, *J* = 7.0 Hz, Ar-H), 7.36 (2H, d, *J* = 6.5 Hz, Ar-H), 7.28 (1H, s, NH). δ_C (125 MHz, $CDCl_3$) 14.2 (CH_3), 22.7, 24.4, 26.1, 29.4,

29.5, 29.6, 31.9, 68.4 (O-CH_2), 114.8, 122.0, 130.9, 156.1 (Ar-C), 168.4 (C=O).

***N*-(4-(dodecyloxy)phenyl)acetamide (9)**. Compound **9** was obtained as a white solid. Yield: 0.62 g (64.0%), m.p: 102 – 103 °C; (Found: C, 75.19; H, 10.39; N, 4.39. $C_{19}H_{31}NO_2$. Requires: C, 75.19; H, 10.41; N, 4.38); ν_{max} (KBr/ cm^{-1}) 3315 (NH), 2918 (CH), 1656 (C=O), 1508 (Ar-C), 1028 (Ar-O). δ_H (500 MHz, $CDCl_3$) 0.87 (3H, t, 1x CH_3), 1.25 – 1.76 (20H, m, 10xCH_2), 2.12 (3H, s, 1xCH_3), 3.91 (2H, t, 1xOCH_2), 6.82 (2H, d, *J* = 9.55 Hz, Ar-H), 7.36 (2H, d, *J* = 9.6 Hz, Ar-H), 7.54 (1H, s, 1xNH). δ_C (125 MHz, $CDCl_3$) 14.2 (CH_3), 22.8, 26.1, 29.4, 29.5, 29.7, 32.0, 68.3 (O-CH_2), 115.1, 122.0, 130.9, 156.1 (Ar-C), 168.5 (C=O).

***N*-(4-(tetradecyloxy)phenyl)acetamide (10)**. Compound **10** was obtained as a white solid. Yield: 0.77 g (74.0%), m.p: 102 – 103 °C; (Found: C, 76.03; H, 10.71; N, 4.03. $C_{20}H_{33}NO_2$. Requires: C, 76.03; H, 10.73; N, 4.03); ν_{max} (KBr/ cm^{-1}) 3317 (NH), 2917(CH), 1655 (C=O), 1509 (Ar-C), 1028 (Ar-O). δ_H (500 MHz, $CDCl_3$) 0.87 (3H, t, 1xCH_3), 1.25 – 1.76 (24H, m, 12xCH_2), 2.13 (3H, s, 1xCH_3), 3.91 (2H, t, 1xOCH_2), 6.83 (2H, d, *J* = 9.55 Hz, Ar-H), 7.36 (2H, d, *J* = 9.6 Hz, Ar-H), 7.27 (1H, s, 1xNH). δ_C (125 MHz, $CDCl_3$) 14.2 (CH_3), 22.7, 26.1, 29.4, 29.5, 29.6, 29.7, 32.0, 68.3 (O-CH_2), 114.8, 122.0, 130.8, 156.1 (Ar-C), 168.3 (C=O).

In vitro Antibacterial Study

The antibacterial activities of *N*-(4-oxy)phenyl)acetamide derivatives **1-10** were determined against *E. coli* and *S. aureus* strains by the Kirby-Bauer disc diffusion method following standard methods recommended by the Clinical and Laboratories Standards Institute (CLSI) for measuring the *in vitro* susceptibility of bacteria to antimicrobial agents used in clinical settings (Nunes *et al*., 2021). The bacteria were grown on media with Mueller-Hinton at 37 °C. The inoculums were stirred at 120 rpm for 18 h. The Mueller Hinton agar was poured into the plate and left for 5 min to solidify. The surface was then inoculated by streaking the swab over the entire agar surface. The plate was rotated approximately 60° each time and swabbed a few times to ensure even inoculum distribution. A 5 mm disc was placed on the surface of the agar plate and was pressed down softly for complete contact. The synthesised compounds **1-10** and paracetamol with a sample volume of 10 µL were impregnated on the discs. Ampicillin was used as a positive control, while DMSO as a negative control. The plates were incubated aerobically at 37 °C for 24 h and the zone of inhibition (halo diameter) was measured by a ruler or calliper.

In silico Molecular Docking Screening

The docking simulation on selected compounds with prominent activities, **1** (*n* = 3), **4** (*n* = 6) **7** (*n* = 9) and **10** (*n* = 14) were carried out using AutoDock Vina 1.1.2 software (Trott & Olson, 2009). The polar hydrogens of the compounds and protein were added with AutoDock Tools 1.5.6 (Abd Halim & Ngaini, 2016) prior to docking with the Autodock Vina program. The cubic grid box of 60 Å size (x, y, z) with a spacing of 0.375 Å was centred while dimensions (x,y,z) were set to 19.667, 19.561, 43.028 and 42.786, 1.624, 23.391 targeted the active site of the *E. coli* and *S. aureus* protein, respectively. The X-ray crystal structure of the DNA gyrase of *E. coli* (PDB entry: 1KZN) and *S. aureus* (PDB entry: 3G7B) was retrieved from Protein Data Bank (http://www.rcsb.pdb.org) (Behera *et al*., 2022; Maahury & Allo, 2021).

In silico Lipinski Rule and Pharmacokinetics ADME

The druglikeness and pharmacokinetic screening on **1-10** were carried out using online software namely SwissADME (Daina *et al*., 2017). The canonical simplified molecular input line entry system (SMILES) notation of the synthesised compounds was used as entry and submitted through the SwissADME tool at http://www.swissadme.ch/index.php whereby the data obtained was analysed by comparing with standard drug ampicillin and parent structure of paracetamol. The druglikeness data follow Lipinski's rule of five bases which the parameter is for the compounds to have a molecular weight (M.W.) <500, octanol–water partition coefficient (Log P) <5, hydrogen bond acceptors (HBA) <10, hydrogen bond donors (HBD) <5 and molar reactivity of 40 – 130 (Al-blewi *et al*., 2018; Adamovich *et al*., 2020). The pharmacokinetics data of **1-10** which is the quantitative study of drug absorption, distribution, metabolism, and excretion (ADME) was extracted based on the compound activity towards cytochrome P450s (CYPs), the

important drug-metabolizing enzymes (Li *et al*., 2019).

RESULTS AND DISCUSSION

Chemistry

The synthesis of *N*-(4-oxy)phenyl)acetamide derivatives **1-10** was carried out via Williamson ether synthesis whereby an alkoxide ion is produced by treating the alcohol group with an organohalide employing a powerful base proceeded with an SN_2 reaction in which an alkoxide ion replaces a halogen ion (Kazemi *et al*., 2013). In this research, 4-hydroxy acetanilide, better known as paracetamol was reacted with a series of bromoalkanes (C_3 – C_{14}) in the presence of a base, K_2CO_3 that aided the polarisation of the phenolic hydroxyl group, thus rendering its nucleophilicity (Javaherian *et al*., 2017). After 48 h of reflux in acetone, compounds **1-10** were obtained with yields of 49-86 % and the synthesis route as illustrated in **Scheme 1**.

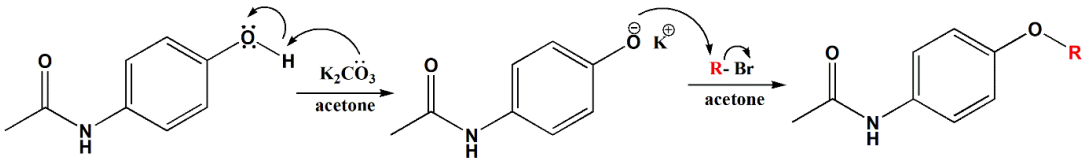

Paracetamol **1-10**

R, 1 = C_3H_7
2 = C_4H_9
3 = C_5H_{11}
4 = C_6H_{13}
5 = C_7H_{15}
6 = C_8H_{17}
7 = C_9H_{19}
8 = $C_{10}H_{21}$
9 = $C_{12}H_{25}$
10 = $C_{14}H_{29}$

Scheme. N-(4-oxy)phenyl)acetamide derivatives **1-10**

The FTIR spectra of **1-10** showed the presence of absorption peaks at 3354 – 3307 cm^{-1} and 2939 – 2917 cm^{-1} attributed to *v* (NH) of acetanilide (El-Rayyes *et al*., 2022) and *v* (CH) of the aliphatic carbon chain, respectively. The strong absorption bands at 1656 – 1655 cm^{-1} were attributed to *v* (C=O) which slight downshift in the frequency than the predicted value of 1700 cm^{-1} due to an intra-molecular hydrogen bond (Abd Halim & Ngaini, 2017). The *v* (Ar-C) absorption band was observed at 1514 – 1507 cm^{-1}.

The confirmation of **1-10** formation was supported by ^1H and ^{13}C NMR spectroscopies. In ^1H NMR spectra, the singlet peak observed at 7.63 – 7.28 ppm was corresponded to CONH (Rahu & Järv, 2020) and the aromatic protons of the compound were represented by two doublets at 7.42 – 7.30 ppm and 6.86 – 6.80 ppm. The successful merging of the alky chain substituent was confirmed by the presence -OCH_2 peak observed at 3.91 – 3.88 ppm and multiple peaks of -CH_2CH_3 chains at 1.76 – 0.80 ppm (Ali & Tomi, 2018). For ^{13}C NMR, the resonance at 168.7 – 168.3 ppm was attributed to C=O, while multiple resonances observed within the 156.1 ppm to 114.8 ppm region were assigned to the aromatic carbon in the structure. The -OCH_2 peak appeared at a higher chemical shift of 69.9 – 68.1 ppm than the alkyl chain -CH_2 resonated at 32.0 – 22.7 ppm due to the downfield effect caused by the electronegative oxygen atom (Abd Halim & Ngaini, 2016; Rahamathullah *et al*., 2018). Whilst, at the most upfield region, a -CH_3 peak was observed at 14.2 – 13.9 ppm.

Antibacterial Activity

The bacteriostatic potential of compounds **1-10** was screened against Gram-negative (*E. coli*) and Gram-positive bacteria (*S. aureus*) employing the Kirby-Bauer disc diffusion method. In this evaluation, ampicillin was chosen as the reference drug (positive control) and paracetamol, a parental compound as a benchmark. The halo diameter of each compound is tabulated in Table 1.

The overall results demonstrated that alkylated series **1-10** showed better inhibition towards *E. coli* than *S. aureus* which was

believed due to the nature of the cell wall of the microorganism (Slavin *et al*., 2017). In comparison to *E. coli*, the cell wall of Gram-positive bacteria such as *S. aureus* is composed of a thicker peptidoglycan layer which limits the diffusion of **1-10** into the membrane decreasing inhibition efficacy (Hamida *et al*., 2020; Hilmi *et al*., 2019). However, notably compounds **7** (*n* = 9) and **10** (*n* = 14) depicted excellent inhibition toward *S. aureus* strains with an inhibition zone of 8.2 ± 0.4 mm and 12.5 ± 0.5 mm, respectively. The latter showed even better inhibition than the ampicillin (11.0 ± 0) drug. This superiority might be due to the structural imitation in terms of carbon chain length of **7** with a pentaglycine bridge and **10** with a pentapeptide stem subsisting in the *S. aureus* peptidoglycan layer (Kim *et al*., 2015; Romaniuk & Cegelski, 2018). The disruption toward those components will rupture the integrity of the cell walls by destroying the peptidoglycan cross-links leading to cell lysis (Loskill *et al.*, 2014; Luo *et al*., 2020).

Focusing on the antibacterial potency of **1-10** toward the *E. coli* strain, all compounds showed inhibitory action with remarkable activity depicted by compounds **1** (*n* = 2), **4** (*n* = 5) and **7** (*n* = 9) exhibited comparable inhibition zone as paracetamol (± 8.0 mm). These foregoing results suggested that compound **1-10** structures having a hydrophilic head and hydrophobic tail owing to the alkyl chain are better suited to permeate through cell membranes in *E. coli* cell walls causing death *(*Kwaśniewska *et al*., 2020; Lin *et al*., 2021). In addition, the alkyl chain heightens the lipophilic character of the compounds increasing the cell permeability into the Gram-negative cell wall that is tightly packed with highly lipophilic lipopolysaccharide (LPS) (Abd Halim & Ngaini, 2016; Kolarič *et al*., 2021).

Table 1. Zone of inhibition of *N*-(4-oxy)phenyl)acetamide derivatives **1-10** against *Escherichia coli* and *Staphylococcus aureus*

Compounds	Halo diameter (mm)	
	E. coli	*S. aureus*
1 (-C_3H_7)	8.1 ± 0.4	5.0 ± 0.0
2 (-C_4H_9)	7.3 ± 0.0	5.5 ± 0.5
3 (-C_5H_{11})	7.3 ± 0.8	5.5 ± 0.5
4 (-C_6H_{13})	8.3 ± 0.4	5.7 ± 0.5
5 (-C_7H_{15})	7.4 ± 0.5	5.0 ± 0.0
6 (-C_8H_{17})	6.7 ± 0.5	5.0 ± 0.0
7 (-C_9H_{19})	7.9 ± 0.5	8.2 ± 0.4
8 (-$C_{10}H_{21}$)	6.9 ± 0.5	5.5 ± 0.5
9 (-$C_{12}H_{25}$)	7.0 ± 0.4	5.0 ± 0.0
10 (-$C_{14}H_{29}$)	7.3 ± 0.4	12.5 ± 0.5
DMSO	5.0 ± 0.0	5.0 ± 0.0
Paracetamol	8.0 ± 0.0	6.0 ± 0.0
Ampicillin	16.0 ± 0.0	11.0 ± 0.0

*5.0 mm is the diameter of the disc

In silico Molecular Docking

To further understand the interaction of compounds **1** (*n* = 3), **4** (*n* = 6), **7** (*n* = 9) and **10** (*n* = 14) with good inhibition capabilities, molecular docking analyses were conducted in comparison to ampicillin as a reference drug and parent compound, paracetamol targeting the DNA gyrase of both studied strains. A DNA gyrase was chosen due to its significance in catalysing the intricate events of DNA supercoiling in prokaryotes, which are in charge of retaining the topological state of bacteria making it a target for antimicrobial drug (Smith & Mondragón, 2021; Jakhar *et al*., 2022). The summary of the interactions is tabulated in Table 2 (*E. coli*) and Table 3 (*S. aureus*).

Table 2. Molecular docking interaction of selected compounds against *Escherichia coli*

Compounds	*E. coli*	
	Binding affinity (kcal/mol)	Binding Residues
Ampicillin	-5.0	TYR26, VAL118, HOH1087
Paracetamol	-4.1	GLU185, ALA188, ARG192, ASP214, HOH1109
1 (-C_3H_7)	-4.5	ARG192, PHE196, TYR218, GLU193
4 (-C_6H_{13})	-4.7	ARG192, HOH1118, PHE196, TYR218, GLU193
7 (-C_9H_{19})	-4.1	ARG192, HOH1082, PHE196, GLU193

Table 3. Molecular docking interaction of selected compounds against *Staphlylococcus aureus*

Compounds	*S. aureus*	
	Binding affinity (kcal/mol)	Binding Residues
Ampicillin	-5.7	THR80, ASN82, GLN66, GLN210
Paracetamol	-4.5	ARG223, TYR192
7(-C_9H_{19})	-4.9	HIS143, THR80, GLU68, LYS170, ASN82, GLN66
10 (-$C_{14}H_{29}$)	-5.5	ARG176, VAL174, TYR141, HIS143, THR80, GLU68, GLN66

The binding affinity of the selected compound was evaluated based on binding free energies (ΔGb, kcal/mol) and the data obtained was in correlation with the *in vitro* antibacterial activity using the disc diffusion procedure discussed earlier. The docking toward *E. coli* protein showed that compound **4** (*n* = 6) scored the highest binding affinity scores of -4.7 kcal/mol (Figure 1d) which is slightly lower than the ampicillin (-5.0 kcal/mol) (Figure 1a**)**. There are several basic residues namely ARG192, HOH1118, TYR218 and GLU193 observed in the vicinity of compound **4** (*n* = 6), remarks a strong electrostatic interaction was involved in the binding process and attributed to high binding affinity scores (Zhou & Pang, 2018). In addition, the phenyl ring in compound **4** (*n* = 6) also strongly enchains to DNA gyrase of *E. coli* through π-π bond interactions (yellow colour cylindrical wireframe) with hydrophobic pockets of PHE196 which subsequently increased the lipophilicity of the compound (Wang *et al*., 2020; Chikhale *et al*., 2021). A similar hydrophobic interaction was also displayed by compound **1** (*n* = 3) with a binding affinity of -4.5 kcal/mol (Figure 1c).

While comparing compound **7** (*n* = 9) with paracetamol which shows a ± 0.1 mm difference in the *in vitro* study previously, there is no difference in terms of their binding affinity as both scored a binding affinity of -4.1 kJ kcal/mol. However, the mode of binding interactions is not identical as the hydroxyl group in paracetamol strongly bound to the DNA gyrase protein through hydrogen bonding with an amine of ASP214 residue (Figure 1b). The presence of hydrogen bonds increases the drug's solubility in water and further promotes interaction between the drug and its biological target (Chen *et al*., 2016; El-Shershaby *et al*., 2021). Whereas, compound **7** (*n* = 9) is linked with the protein through electrostatic interaction with ARG192, HOH1082, PHE196, and GLU193 residues (Figure 1e).

The docking of the selected compounds with DNA gyrase of *S. aureus* on the other hand showed that paracetamol scored a lower binding affinity of -4.5 kJ kcal/mol (Figure 2b) in line with the *in vitro* data showing slight inhibition. Whilst, compound **10** (*n* = 14) with the biggest inhibition zone scored a binding value of -5.5 kcal/mol (Figure 2d) which is slightly lower than the ampicillin of -5.7 kcal/mol (Figure 2a). Both compounds, however, possessed similar modes of binding action by strong electrostatic interaction with the protein as multiple residues are observed in proximity disrupting the cell stability (Halperin *et al*., 2004; Zhou & Pang, 2018). Even though it is not reflected in terms of binding affinity value, there are more residues for compound **10** (*n* = 14) namely ARG176, VAL174, TYR141, HIS143, THR80, GLU68 and GLN66 than ampicillin binding to only THR80, ASN82, GLN66 and GLN210 residues reasoned the better inhibition of **10** than ampicillin in *in vitro* study. Likewise, compound **7** (*n* = 9) interacted with residues like HIS143, THR80, GLU68, LYS170, ASN82 and GLN66 giving docked scores of -4.9 kcal/mol (Figure 2c).

Drug likeness and pharmacokinetic properties – ADME profile

For a newly developed compound to be a drug candidate, it is important to determine its drug-likeness referring to Lipinski's rules of five (Parameter: molecular weight, hydrogen donor, hydrogen acceptor, lipophilicity and molar refractivity) (Adamovich *et al*., 2020; Mendie & Hemalatha, 2022) and the pharmacokinetic properties catering for the absorption, distribution, metabolism and excretion detailed of a drug (Bocci *et al*., 2017; Kar & Leszczynski, 2020). This is a crucial step in drug design and drug discovery stages aiming to increase the likelihood that a chemical will enter and succeed in clinical trials (Jia *et al*., 2020). In this study, the screening was conducted employing SwissADME software available on the platform (Daina *et al*., 2017).

The data obtained showed that all alkylated paracetamol derivatives except **10** (*n*=14) complied with Lipinski's rule indicating the synthesised series exhibit high drug-likeness and potential to be orally active (Al-blewi *et al*., 2018) as tabulated in Table 4. Compound **10** (*n*=14) violated the parameter MlogP ≤ 4.15 revealing the low lipophilicity and high hydrophobic nature of the compound reflecting poor oral bioavailability (Shady *et al*., 2020).

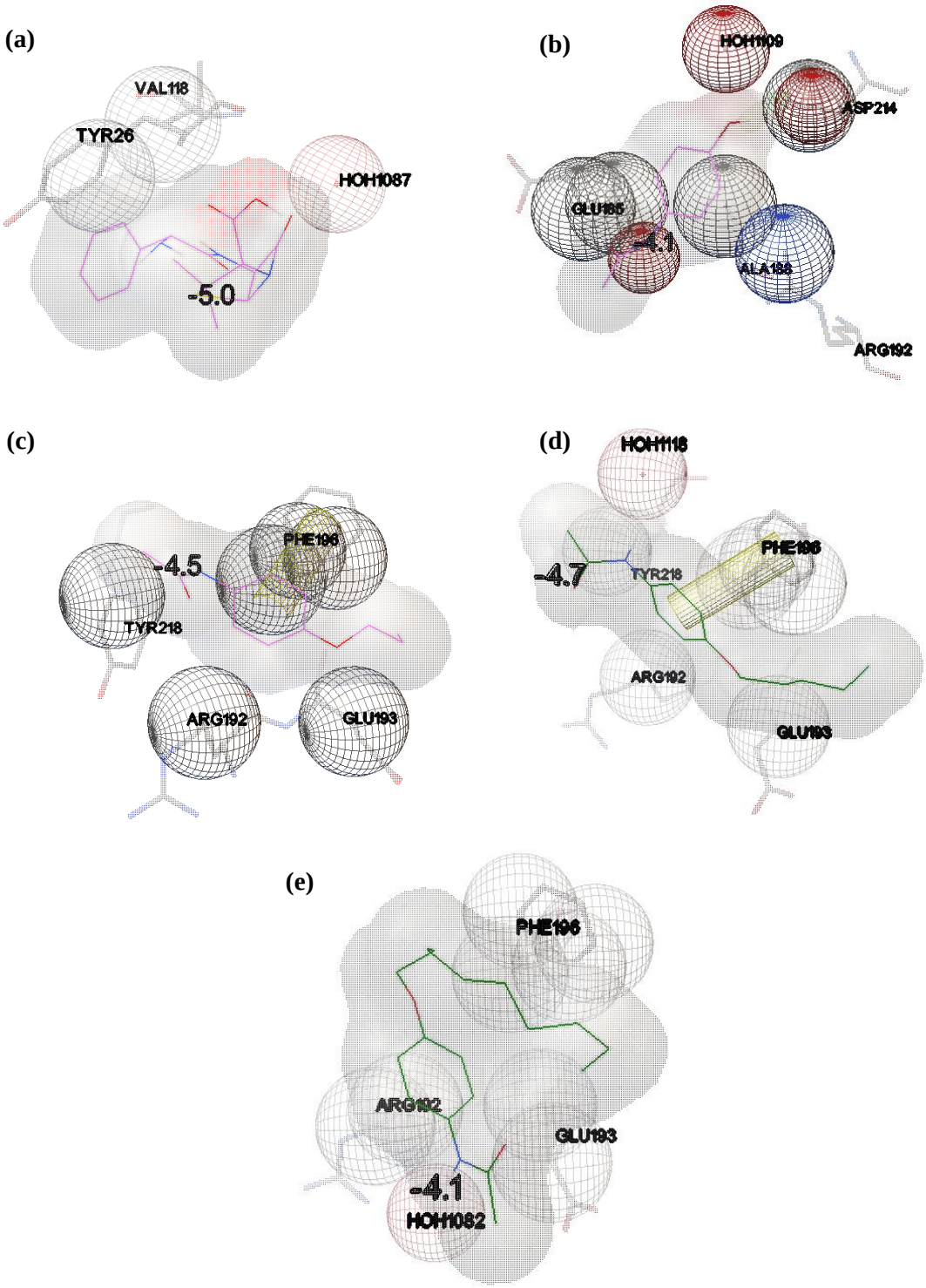

Figure 1. Docking visualisation of (a) ampicillin, (b) paracetamol, (c) **1** (*n* = 3), (d) **4** (*n* = 6) and (e) **7** (*n* = 9) towards DNA gyrase of *E. coli* (PDB entry: 1KZN)

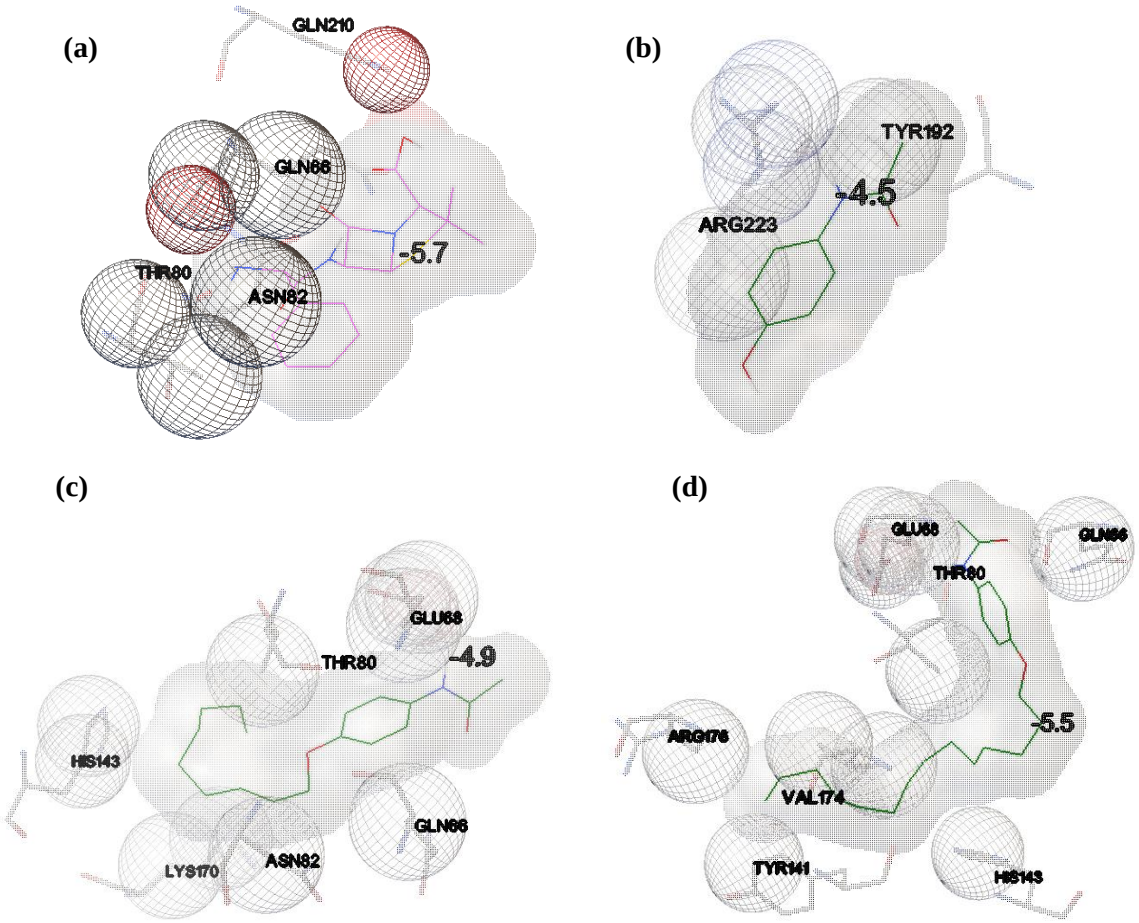

Figure 2. Docking visualisation of (a) ampicillin, (b) paracetamol, (c) **7** (*n* = 9) and (d) **10** (*n* = 14) towards DNA gyrase of *Staphlyloccus aureus* (PDB entry: 3G7B)

Table 4. Lipinski's Rule of Five for compound **1-10**

Molecule	Lipinski rule violation	MW (≤ 500 Da)	H-bond acceptors (≤ 5)	H-bond donors (≤ 10)	Molar Refractivity (40 - 130)	MLOGP (≤4.15)
Ampicilin	No	349.40	5	3	92.56	0.75
Paracetamol	No	151.16	2	2	42.78	0.91
1 (-C_3H_7)	No	193.24	2	1	56.86	1.83
2 (-C_4H_9)	No	207.27	2	1	61.67	2.11
3 (-C_5H_{11})	No	221.30	2	1	66.47	2.38
4 (-C_6H_{13})	No	235.32	2	1	71.28	2.64
5 (-C_7H_{15})	No	249.35	2	1	76.09	2.90
6 (-C_8H_{17})	No	263.38	2	1	80.90	3.15
7 (-C_9H_{19})	No	277.40	2	1	85.70	3.39
8 (-$C_{10}H_{21}$)	No	291.43	2	1	90.51	3.63
9 (-$C_{12}H_{25}$)	No	319.48	2	1	100.12	4.09
10 (-$C_{14}H_{29}$)	Yes; 1 violation: MLOGP>4.15	347.53	2	1	109.74	4.53

The pharmacokinetic profile on N-(4-oxy)phenyl)acetamide derivatives **1–10** revealed that all compounds have a bioavailability score of 0.55 and possessed high GI absorption predicting the suitability of the compound to be administered orally and acting at the intended target site of action to deliver a good therapeutic effect (Xue *et al*., 2022). In addition, similar to the parent compound paracetamol, the series except for **10** (*n*=14) are able to permeate the blood-brain barrier (BBB). Having the capability to cross BBB for newly developed antibacterial drugs is a significant finding in the treatment of the central nervous

system (CNS) infected pathogen disorder (Nau *et al*., 2010; Sullins & Abdel-Rahman, 2013; Bagchi *et al*., 2019). Other remarkable pharmacokinetic properties exhibited by compounds **1-10** are the CYP1A2 inhibition that is not displayed by both ampicillin and paracetamol. CYP1A2 is an enzyme that is majorly expressed in the liver and the ability to suppress this enzyme is predicted to increase drug adsorption concentration into plasma hence decreasing substrate clearance or excretion and enhancing the therapeutic effect (Ayano, 2016; Mar *et al*., 2022). Apart from the above discussion, as tabulated in Table 5, each of the synthesised compounds showed multi-inhibitory action to cytochrome P450 (CYP) enzymes underlining its versatile metabolism action aside from lowering drug-drug interaction (DDI) interactions (Bocci *et al*., 2017).

Table 5. Pharmacokinetic profile of N-(4-oxy)phenyl)acetamide derivatives **1–10**

Molecule	GI absorption	BBB permeant	Pgp substrate	CYP1A2 inhibitor	CYP2C19 inhibitor	CYP2C9 inhibitor	CYP2D6 inhibitor	CYP3A4 inhibitor	Bioavailability Score
Ampicillin	Low	No	No	No	No	No	No	No	0.55
Paracetamol	High	Yes	No	No	No	No	No	No	0.55
1 (-C_3H_7)	High	Yes	No	Yes	No	No	No	No	0.55
2 (-C_4H_9)	High	Yes	No	Yes	No	No	Yes	No	0.55
3 (-C_5H_{11})	High	Yes	No	Yes	No	No	Yes	No	0.55
4 (-C_6H_{13})	High	Yes	No	Yes	Yes	No	Yes	No	0.55
5 (-C_7H_{15})	High	Yes	No	Yes	Yes	No	Yes	No	0.55
6 (-C_8H_{17})	High	Yes	No	Yes	Yes	No	Yes	No	0.55
7 (-C_9H_{19})	High	Yes	No	Yes	Yes	Yes	Yes	No	0.55
8 (-$C_{10}H_{21}$)	High	Yes	No	Yes	No	Yes	Yes	No	0.55
9 (-$C_{12}H_{25}$)	High	Yes	No	Yes	No	Yes	Yes	Yes	0.55
10 (-$C_{14}H_{29}$)	High	No	No	Yes	No	No	Yes	Yes	0.55

CONCLUSION

The alkylated paracetamol derivatives **1-10** were successfully synthesised with promising antibacterial potential. According to the *in vitro* results, compounds **1** (*n* = 3), **4** (*n* = 6) and **7** (*n* = 9) had good antibacterial activity against Gram-negative (*E. coli*), whereas compounds **7** (*n* = 9) and **10** (*n* = 14) had excellent activity towards Gram-positive (*S. aureus*). The biological effect is significantly enhanced by the presence of the alkyl chain, which was confirmed by the binding affinity discovered through molecular docking studies. In addition, compounds **1-10** exhibited a bioavailability score of 0.55 apart from compliances with Lipinski's rule on the drug-likeness and favourable ADME pharmacokinetics profile. Overall, this study provided a thorough analysis of the potential of the series as an antibacterial agent for pharmaceutical applications.

ACKNOWLEDGEMENTS

The authors would like to thank Universiti Malaysia Sarawak for the Small Grant Scheme research funds F07/PILOT/2111/2021.

REFERENCES

Abd Halim, A.N. & Ngaini, Z. (2016). Synthesis and bacteriostatic activities of bis(thiourea) derivatives with variable chain length. *Journal of Chemistry*, 2016. DOI: 10.1155/2016/2739832

Abd Halim, A.N. & Ngaini, Z. (2017). Synthesis and characterization of halogenated bis(acylthiourea) derivatives and their antibacterial activities. *Phosphorus, Sulfur and Silicon and the Related Elements*, 192(9): 1012-1017. DOI: 10.1080/1042 6507.2017.1315421

Adamovich, S.N., Kondrashov, E.V., Ushakov, I.A., Shatokhina, N.S., Oborina, E.N., Vashchenko, A.V., Belovezhets, L.A., Rozentsveig, I.B. & Verpoort, F. (2020). Isoxazole derivatives of silatrane: synthesis, characterization, in silico ADME profile, prediction of potential pharmacological activity and evaluation of antimicrobial action. *Applied Organometallic Chemistry*, 34(12): e5976. DOI: 10.1002/aoc.5976

Ahmad, A., Husain, A., Khan, S.A., Mujeeb, M. & Bhandari, A. (2016). Synthesis, antimicrobial and antitubercular activities of some novel pyrazoline derivatives Antimicrobial and antitubercular activities of novel pyrazoline derivatives. *Journal of Saudi Chemical Society*, 20(5): 577-584. DOI:

10.1016/j.jscs.2014.12.004

Al-blewi, F.F., Almehmadi, M.A., Aouad, M.R., Bardaweel, S.K., Sahu, P.K., Messali, M., Rezki, N. & El Ashry, E.S.H. (2018). Design, synthesis, ADME prediction and pharmacological evaluation of novel benzimidazole-1,2,3-triazole-sulfonamide hybrids as antimicrobial and antiproliferative agents. *Chemistry Central Journal*, 12(1): 1-14. DOI: 10.1186/s13065-018-0479-1

Ali, G.Q. & Tomi, I.H.R. (2018). Synthesis and characterization of new mesogenic esters derived from 1,2,4-oxadiazole and study the effect of alkoxy chain length in their liquid crystalline properties. *Liquid Crystals*, 45(3): 421-430. DOI: 10.1080/02678292.2017.1338767

Alisi, M.A., Brufani, M., Cazzolla, N., Ceccacci, F., Dragone, P., Felici, M., Furlotti, G., Garofalo, B., La Bella, A., Lanzalunga, O., Leonelli, F., Marini Bettolo, R., Maugeri, C., Migneco, L.M. & Russo, V. (2012). DPPH radical scavenging activity of paracetamol analogues. *Tetrahedron*, 68(49): 10180-10187. DOI: 10.1016/j.tet.2012.09.098

Ardean, C., Davidescu, C.M., Neme, N.S., Negrea, A., Ciopec, M., Duteanu, N., Negrea, P., Dida-Seiman, D. & Musta, V. (2021). Factors influencing the antibacterial activity of chitosan and chitosan modified by functionalization. *International Journal of Molecular Sciences*, 22(7449): 1-28. DOI: 10.3390/ijms22147449

Ayano, G. (2016). Psychotropic medications metabolized by Cytochromes P450 (CYP) 2D6 enzyme and relevant drug interactions. *Clinical Pharmacology and Biopharmaceutics*, 05(04): 2-5. DOI: 10.4172/2167-065x.1000162

Babamale, H.F., Sangeetha, T., Tan, J.S., & Yam, W.S. (2021). Synthesis and characterization of azobenzene derivatives and azobenzene-imidazolium conjugates with selective antimicrobial potential. *Journal of Molecular Structure*, 1232: 130049. DOI: 10.1016/j.molstruc.2021.130049

Bagchi, S., Chhibber, T., Lahooti, B., Verma, A., Borse, V. & Jayant, R.D. (2019). *In-vitro* blood-brain barrier models for drug screening and permeation studies: An overview. *Drug Design, Development and Therapy*, 13: 3591-3605. DOI: 10.2147/DDDT.S218708

Barbolosi, D., Ciccolini, J., Lacarelle, B., Barlési, F. & André, N. (2016). Computational oncology-mathematical modelling of drug regimens for precision medicine. *Nature Reviews Clinical Oncology*, 13(4): 242-254. DOI: 10.1038/nrclinonc.2015.204

Batool, M., Ahmad, B. & Choi, S. (2019). A structure-based drug discovery paradigm. *International Journal of Molecular Sciences*, 20(11): 2783. DOI: 10.3390/ijms20112783

Begum, S., Harisree, G.P. & Anjum, M.S.R. (2023). A short review on biological activities of paracetamol derivatives. *International Journal of Pharmaceutical Sciences and Nanotechnology*, 16(1): 6309-6324. DOI: 10.37285/ijpsn.2023.16.1.5

Behera, S., Dash, P.P., Bishoyi, A.K., Dash, K., Mohanty, P., Sahoo, C.R., Padhy, R.N., Mishra, M., Ghosh, B.N., Sahoo, H. & Jali, B.R. (2022). Protein interactions, molecular docking, antimicrobial and antifungal studies of terpyridine ligands. *Journal of Biomolecular Structure and Dynamics*, 41(20): 11274-11285. DOI: 10.1080/07391102.2022.2161012

Bocci, G., Carosati, E., Vayer, P., Arrault, A., Lozano, S. & Cruciani, G. (2017). ADME-Space: A new tool for medicinal chemists to explore ADME properties. *Scientific Reports*, 7(1): 25-27. DOI: 10.1038/s41598-017-06692-0

Chen, D., Oezguen, N., Urvil, P., Ferguson, C., Dann, S.M. & Savidge, T.C. (2016). Regulation of protein-ligand binding affinity by hydrogen bond pairing. *Science Advances*, 2(3): e1501240. DOI: 10.1126/sciadv.1501240

Chikhale, R.V., Gurav, S.S., Patil, R.B., Sinha, S.K., Prasad, S.K., Shakya, A., Shrivastava, S.K., Gurav, N.S. & Prasad, R.S. (2021). Sars-cov-2 host entry and replication inhibitors from Indian ginseng: an in-silico approach. *Journal of Biomolecular Structure and Dynamics*, 39(12): 4510-4521. DOI: 10.1080/07391102.2020.1778539

Daina, A., Michielin, O. & Zoete, V. (2017). SwissADME: A free web tool to evaluate pharmacokinetics, drug-likeness and medicinal chemistry friendliness of small molecules. *Scientific Reports*, 7: 1-13. DOI: 10.1038/srep42717

Deore, A.B., Dhumane, J.R., Wagh, R. & Sonawane, R. (2019). The stages of drug discovery and development process. *Asian Journal of Pharmaceutical Research and Development*, 7(6): 62-67. DOI: 10.22270/ajprd.v7i6.616

El-Rayyes, A., Soliman, A.M. & Saeed, A. (2022). Synthesis and anticancer evaluation of new thiazole and thiadiazole derivatives bearing

acetanilide moiety. *Russian Journal of General Chemistry*, 92(10): 2132-2144. DOI: 10.1134/S1070363222100267

El-Shershaby, M.H., El-Gamal, K.M., Bayoumi, A.H., El-Adl, K., Alswah, M., Ahmed, H.E.A., Al-Karmalamy, A.A. & Abulkhair, H.S. (2021). The antimicrobial potential and pharmacokinetic profiles of novel quinoline-based scaffolds: synthesis andin silicomechanistic studies as dual DNA gyrase and DHFR inhibitors. *New Journal of Chemistry*, 45(31): 13986-14004. DOI: 10.1039/d1nj02838c

Farha, M.A. & Brown, E.D. (2019). Drug repurposing for antimicrobial discovery. *Nature Microbiology*, 4(4): 565-577. DOI: 10.1038/s41564-019-0357-1

Gao, W., Han, X., Li, Y., Zhou, Z., Wang, J., Shi, R., Jiao, J., Qi, Y., Zhou, Y. & Zhao, J. (2022). Modification strategies for improving antibacterial properties of polyetheretherketone. *Journal of Applied Polymer Science*, 139(36): 1-12. DOI: 10.1002/app.52847

Halperin, I., Wolfson, H. & Nussinov, R. (2004). Protein-protein interactions: Coupling of structurally conserved residues and of hot spots across interfaces. Implications for docking. *Structure*, 12(6): 1027-1038. DOI: 10.1016/j.str.2004.04.009

Hamida, R.S., Ali, M.A., Goda, D.A., Khalil, M.I. & Al-Zaban, M.I. (2020). Novel biogenic silver nanoparticle-induced reactive oxygen species inhibit the biofilm formation and virulence activities of methicillin-resistant *S. aureus* (MRSA) strain. *Frontiers in Bioengineering and Biotechnology*, 8: 1-14. DOI: 10.3389/fbioe.2020.00433

Hilmi, B., Bustami, Y., Trongsatitkul, T. & Abdul Hamid, Z.A. (2019). The effect of natural antimicrobial agents on *S. aureus* and *E. coli* growth. *Journal of Physical Science*, 30: 55-63. DOI: 10.21315 /JPS2019.30.S2.5

Jakhar, R., Khichi, A., Kumar, D., Dangi, M. & Chhillar, A.K. (2022). Discovery of Novel inhibitors of bacterial DNA gyrase using a QSAR-based approach. *ACS Omega*, 7(36): 32665-32678. DOI: 10.1021/acsomega.2c04310

Javaherian, M., Kazemi, F., Ayati, S.E., Davarpanah, J. & Ramdar, M. (2017). A tandem scalable microwave-assisted Williamson alkyl aryl ether synthesis under mild conditions. *Organic Chemistry Research*, 3(1): 73-85.

Jia, C.Y., Li, J.Y., Hao, G.F. & Yang, G.F. (2020). A drug-likeness toolbox facilitates ADMET study in drug discovery. *Drug Discovery Today*: 25(1): 248-258. DOI: 10.1016/j.drudis.2019.10.014

Kar, S. & Leszczynski, J. (2020). Open access *in silico* tools to predict the ADMET profiling of drug candidates. *Expert Opinion on Drug Discovery*, 15(12): 1473-1487. DOI: 10.1080/ 17460441.2020.1798926

Kazemi, M., Noori, Z., Kohzadi, H., Sayadi, M. & Kazemi, A. (2013). A mild and efficient procedure for the synthesis of ethers from various alkyl halides. *Iranian Chemical Communication*, 1(841): 43-50.

Kim, S.J., Chang, J. & Singh, M. (2015). Peptidoglycan architecture of Gram-positive bacteria by solid-state NMR. *Biochimica et Biophysica Acta - Biomembranes*, 1848(1): 350-362. DOI: 10.1016/j.bbamem.2014.05.031

Kolarič, A., Kokot, M., Hrast, M., Weiss, M., Zdovc, I., Trontelj, J., Žakelj, S., Anderluh, M. & Minovski, N. (2021). A fine-tuned lipophilicity/hydrophilicity ratio governs antibacterial potency and selectivity of bifurcated halogen bond-forming NBTIs. *Antibiotics*, 10(7): 862. DOI: 10.3390/antibiotics10070862

Kumar, K.S., Rao, A.L., Sri, M.B., Pravallika, M., Kalyani, M. & Ramudu, K.S. (2018). Synthesis of paracetamol derivatives as mannich bases and their antibacterial activity. *Journal of Pharmaceutical and Health Sciences*, 6(2): 169-176.

Kwaśniewska, D., Chen, Y.L. & Wieczorek, D. (2020). Biological activity of quaternary ammonium salts and their derivatives. *Pathogens*, 9(6): 1-12. DOI: 10.3390/pathogens9060459

Li, Y., Meng, Q., Yang, M., Liu, D., Hou, X., Tang, L., Wang, X., Lyu, Y., Chen, X., Liu, K., Yu, A. M., Zuo, Z. & Bi, H. (2019). Current trends in drug metabolism and pharmacokinetics. *Acta Pharmaceutica Sinica B*, 9(6): 1113-1144. DOI: 10.1016/j.apsb.2019.10.001

Lin, B., Hung, A., Singleton, W., Darmawan, K.K., Moses, R., Yao, B., Wu, H., Barlow, A., Sani, M., Sloan, A.J., Hossain, M.A., Wade, J.D., Hong, Y., O'Brien-Simpson, N.M. & Li, W. (2023). The effect of tailing lipidation on the bioactivity of antimicrobial peptides and their aggregation tendency. *Aggregate*, 4(4): 1-15. DOI: 10.1002/ agt2.329

Lin, C., Wang, Y., Le, M., Chen, K.F. & Jia, Y.G. (2021). Recent progress in bile acid-based antimicrobials. *Bioconjugate Chemistry*, 32(3):

395-410. DOI: 10.1021/acs.bioconjchem .0c00642

Long, Y., Jin, Z., Li, L., Zhang, M., Hu, L., Shen, D. & Ruan, J. (2020). Dechlorination of chlorotoluene rectification residual liquid (CRRL) by using Williamson ether synthesis (WES) method. *Environmental Science and Pollution Research*, 27(12): 14198-14206. DOI: 10.1007/s11356-020-07957-4

Loskill, P., Pereira, P.M., Jung, P., Bischoff, M., Herrmann, M., Pinho, M.G. & Jacobs, K. (2014). Reduction of the peptidoglycan crosslinking causes a decrease in stiffness of the *S. aureus* cell envelope. *Biophysical Journal*, 107(5): 1082-1089. DOI: 10.1016/j.bpj.2014.07.029

Luo, Z., Yue, S., Chen, T., She, P., Wu, Y. & Wu, Y. (2020). Reduced growth of *Staphylococcus aureus* under high glucose conditions is associated with decreased pentaglycine expression. *Frontiers in Microbiology*, 11: 1-11. DOI: 10.3389/fmicb.2020.537290

Maahury, M.F. & Allo, V.L. (2021). The computational calculation and molecular docking of aeroplysinin-1 as antibacterial. *Indonesian Journal of Chemical Research*, 9(2): 124-128. DOI: 10.30598//ijcr.2020.9-mir

Mar, P.L., Gopinathannair, R., Gengler, B.E., Chung, M.K., Perez, A., Dukes, J., Ezekowitz, M.D., Lakkireddy, D., Lip, G.Y.H., Miletello, M., Noseworthy, P.A., Reiffel, J., Tisdale, J.E. & Olshansky, B. (2022). Drug interactions affecting oral anticoagulant use. *Circulation: Arrhythmia and Electrophysiology*, 15(6): E007956. DOI: 10.1161/CIRCEP.121.007956

Mehta, D., Saini, V., Aggarwal, B., Khan, A. & Bajaj, A. (2021). Unlocking the bacterial membrane as a therapeutic target for next-generation antimicrobial amphiphiles. *Molecular Aspects of Medicine*, 81: 100999. DOI: 10.1016/j.mam .2021.100999

Mendie, L.E. & Hemalatha, S. (2022). Molecular docking of phytochemicals targeting GFRs as therapeutic sites for cancer: an in silico study. *Applied Biochemistry and Biotechnology*, 194(1): 215-231. DOI: 10.1007/s12010-021-03791-7

Moo, C.L., Yang, S.K., Yusoff, K., Ajat, M., Thomas, W., Abushelaibi, A., Lim, S.H.E. & Lai, K.S. (2019). Mechanisms of antimicrobial resistance (AMR) and alternative approaches to overcome AMR. *Current Drug Discovery Technologies*, 17(4): 430-447. DOI: 10.2174/ 1570163816666190304122219

Nau, R., Sörgel, F. & Eiffert, H. (2010). Penetration of drugs through the blood-cerebrospinal fluid/blood-brain barrier for treatment of central nervous system infections. *Clinical Microbiology Reviews*, 23(4): 858-883. DOI: 10.1128/CMR. 00007-10

Nunes, D.O.S., Vinturelle, R., Martins, F.J., dos Santos, T.F., Valverde, A.L., Ribeiro, C.M.R., Castro, H.C. & Folly, E. (2021). Biotechnological potential of eugenol and thymol derivatives against *Staphylococcus aureus* from bovine mastitis. *Current Microbiology*, 78(5): 1846-1855. DOI: 10.1007/s00284-021-02344-9

Odžak, R., Crnˇ, D., Sablji, A., Krce, L., Paladin, A. & Primoži ˇ, I. (2023). *Further Study of the Polar Group ' s Influence on the Antibacterial Activity of the 3-Substituted Quinuclidine Salts with Long Alkyl Chains*.

Przybyła, G.W., Szychowski, K.A. & Gmiński, J. (2021). Paracetamol – An old drug with new mechanisms of action. *Clinical and Experimental Pharmacology and Physiology*, 48(1): 3-19. DOI: 10.1111/1440-1681.13392

Rahamathullah, R., Keemi, L. & Khairul, W.M. (2018). Assessment on heck-immine derivatives as organic semiconductor materials. *Makara Journal of Technology*, 21(3): 115. DOI: 10.7454/mst.v21i3.3368

Rahu, I. & Järv, J. (2020). Solvent -free synthesis of molecular bromine and its application for *in situ* bromination of aromatic compounds. *Proceedings of the Estonian Academy of Sciences*, 69(3): 208-214. DOI: 10.3176/ proc.2020.3.04

Ramanjaneyulu, K., Bindhu, J., Babu, R., Prasad, Y., Naaz, T., Ranjani, P. & Gouthami, P. (2019). Design, synthesis and characterization of novel paracetamol derivatives to target breast cancer. *Indian Journal of Chemistry -Section B (IJC-B)*, 58(11): 1257-1272.

Refat, M.S., Mohamed, G.G., El-Sayed, M.Y., Killa, H.M.A. & Fetooh, H. (2017). Spectroscopic and thermal degradation behavior of Mg(II), Ca(II), Ba(II) and Sr(II) complexes with paracetamol drug. *Arabian Journal of Chemistry*, 10: S2376-S2387. DOI: 10.1016/j.arabjc.2013.08.017

Romaniuk, J.A.H. & Cegelski, L. (2018). Peptidoglycan and teichoic acid levels and alterations in *S. aureus* by cell-wall and whole-cell nuclear magnetic resonance. *Biochemistry*, 57(26): 3966-3975. DOI: 10.1021 /acs.biochem.8b00495

Sahariah, P., Benediktssdóttir, B.E., Hjálmarsdóttir, M.A., Sigurjonsson, O.E., Sørensen, K.K., Thygesen, M.B., Jensen, K.J. & Másson, M. (2015). Impact of chain length on antibacterial activity and hemocompatibility of quaternary N-alkyl and N, N-dialkyl chitosan derivatives. *Biomacromolecules*, 16(5): 1449-1460. DOI: 10.1021/acs.biomac.5b00163

Sathe, P.S., Rajput, J.D., Gunaga, S.S., Patel, H.M. & Bendre, R.S. (2019). Synthesis, characterization, and antioxidant activity of thymol-based paracetamol analogues. *Research on Chemical Intermediates*, 45(11): 5487-5498. DOI: 10.1007/s11164-019-03914-0

Shady, N.H., Khattab, A.R., Ahmed, S., Liu, M., Quinn, R.J., Fouad, M.A., Kamel, M.S., Muhsinah, A., Krischke, M., Mueller, M.J. & Abdelmohsen, U.R. (2020). Hepatitis c virus ns3 protease and helicase inhibitors from red sea sponge (Amphimedon) species in green siz silver nanoparticles assisted by in silico modeling and metabolic profiling. *International Journal of Nanomedicine*, 15: 3377-3389. DOI: 10.2147/ IJN.S233766

Slavin, Y.N., Asnis, J., Hńfeli, U.O. & Bach, H. (2017). Metal nanoparticles: understanding the mechanisms behind antibacterial activity. *Journal of Nanobiotechnology*, 5: 1-20.

Smith, E.M. & Mondragón, A. (2021). Basic residues at the C-gate of DNA gyrase are involved in DNA supercoiling. *Journal of Biological Chemistry*, 297(2): 101000. DOI: 10.1016/j.jbc.2021.101000

Srabovic, M., Huremovic, M., Catovic, B. & Muratovic, S. (2017). Design synthesis and crystallization of acetaminophen. *Journal of Chemical, Biological and Physical Sciences*, 7: 218-230.

Sullins, A.K. & Abdel-Rahman, S.M. (2013). Pharmacokinetics of antibacterial agents in the CSF of children and adolescents. *Pediatric Drugs*, 15(2): 93-117. DOI: 10.1007/s40272-013-0017-5

Trott, O. & Olson, A.J. (2009). AutoDock Vina: improving the speed and accuracy of docking with a new scoring function, efficient optimization, and multithreading. *Journal of Computational Chemistry*, 31(2): 455-461. DOI: 10.1002/jcc.21334

Wang, Y., Liu, M. & Gao, J. (2020). Enhanced receptor binding of SARS-CoV-2 through networks of hydrogen-bonding and hydrophobic interactions. *Proceedings of the National Academy of Sciences of the United States of America*, 117(25): 13967-13974. DOI: 10.1073/pnas.2008209117

Xue, S., Wang, X., Wang, L., Xu, W., Xia, S., Sun, L., Wang, S., Shen, N., Yang, Z., Huang, B., Li, S., Cao, C., Calcul, L., Sun, X., Lu, L., Cai, J. & Jiang, S. (2022). A novel cyclic γ-AApeptide-based long-acting pan-coronavirus fusion inhibitor with potential oral bioavailability by targeting two sites in spike protein. *Cell Discovery*, 8:88. DOI: 10.1038/s41421-022-

Yearty, K.L., Maynard, R.K., Cortes, C.N. & Morrison, R.W. (2020). A multioutcome experiment for the Williamson ether synthesis. *Journal of Chemical Education*, 97(2): 578-581. DOI: 10.1021/acs.jchemed.9b00503

Zhou, H.X. & Pang, X. (2018). Electrostatic interactions in protein structure, folding, binding, and condensation. *Chemical Reviews*, 118(4): 1691-1741.